REFERENCES AND NOTES

1. D. L. Schacter, D. R. Addis, *Philos. Trans. R. Soc. Lond. B Biol. Sci.* **364**, 1245–1253 (2009).
2. R. L. Buckner, D. C. Carroll, *Trends Cogn. Sci.* **11**, 49–57 (2007).
3. E. R. Wood, P. A. Dudchenko, R. J. Robitsek, H. Eichenbaum, *Neuron* **27**, 623–633 (2000).
4. I. Lee, A. L. Griffin, E. A. Zilli, H. Eichenbaum, M. E. Hasselmo, *Neuron* **51**, 639–650 (2006).
5. D. M. Smith, S. J. Mizumori, *J. Neurosci.* **26**, 3154–3163 (2006).
6. H. T. Ito, S.-J. Zhang, M. P. Witter, E. I. Moser, M.-B. Moser, *Nature* **522**, 50–55 (2015).
7. J. Ferbinteanu, M. L. Shapiro, *Neuron* **40**, 1227–1239 (2003).
8. T. I. Brown, M. E. Hasselmo, C. E. Stern, *Hippocampus* **24**, 819–839 (2014).
9. T. I. Brown, C. E. Stern, *Cereb. Cortex* **24**, 1906–1922 (2014).
10. T. I. Brown, R. S. Ross, J. B. Keller, M. E. Hasselmo, C. E. Stern, *J. Neurosci.* **30**, 7414–7422 (2010).
11. T. I. Brown, R. S. Ross, S. M. Tobyne, C. E. Stern, *Neuroimage* **60**, 1316–1330 (2012).
12. T. I. Brown, A. S. Whiteman, I. Aselcioglu, C. E. Stern, *J. Neurosci.* **34**, 2314–2320 (2014).
13. M. E. Hasselmo, H. Eichenbaum, *Neural Netw.* **18**, 1172–1190 (2005).
14. M. E. Hasselmo, *Neurobiol. Learn. Mem.* **92**, 559–573 (2009).
15. M. E. Hasselmo, C. E. Stern, *Neuroimage* **85**, 656–666 (2014).
16. A. Johnson, A. D. Redish, *J. Neurosci.* **27**, 12176–12189 (2007).
17. A. M. Wikenheiser, A. D. Redish, *Nat. Neurosci.* **18**, 289–294 (2015).
18. D. R. Addis, A. T. Wong, D. L. Schacter, *Neuropsychologia* **45**, 1363–1377 (2007).
19. M. A. A. van der Meer, A. Johnson, N. C. Schmitzer-Torbert, A. D. Redish, *Neuron* **67**, 25–32 (2010).
20. P. Byrne, S. Becker, N. Burgess, *Psychol. Rev.* **114**, 340–375 (2007).
21. N. Burgess, S. Becker, J. A. King, J. O'Keefe, *Philos. Trans. R. Soc. London B Biol. Sci.* **356**, 1493–1503 (2001).
22. N. Ramnani, A. M. Owen, *Nat. Rev. Neurosci.* **5**, 184–194 (2004).
23. H. J. Spiers, S. J. Gilbert, *Front. Hum. Neurosci.* **9**, 125 (2015).
24. J. F. Miller *et al.*, *Science* **342**, 1111–1114 (2013).
25. A. D. Ekstrom *et al.*, *Nature* **425**, 184–188 (2003).
26. L. R. Howard *et al.*, *Curr. Biol.* **24**, 1331–1340 (2014).
27. K. R. Sherrill *et al.*, *J. Neurosci.* **33**, 19304–19313 (2013).
28. H. J. Spiers, E. A. Maguire, *Hippocampus* **17**, 618–626 (2007).
29. C. F. Doeller, C. Barry, N. Burgess, *Nature* **463**, 657–661 (2010).
30. M. J. Chadwick, A. E. J. Jolly, D. P. Amos, D. Hassabis, H. J. Spiers, *Curr. Biol.* **25**, 87–92 (2015).
31. V. Sulpizio, G. Committeri, G. Galati, *Front. Hum. Neurosci.* **8**, 716 (2014).
32. D. Hassabis *et al.*, *Curr. Biol.* **19**, 546–554 (2009).
33. S. A. Marchette, L. K. Vass, J. Ryan, R. A. Epstein, *Nat. Neurosci.* **17**, 1598–1606 (2014).
34. S. A. Marchette, L. K. Vass, J. Ryan, R. A. Epstein, *J. Neurosci.* **35**, 14896–14908 (2015).
35. S. McKenzie, N. T. M. Robinson, L. Herrera, J. C. Churchill, H. Eichenbaum, *J. Neurosci.* **33**, 10243–10256 (2013).
36. J. C. Liang, A. D. Wagner, A. R. Preston, *Cereb. Cortex* **23**, 80–96 (2013).
37. E. M. Aminoff, K. Kveraga, M. Bar, *Trends Cogn. Sci.* **17**, 379–390 (2013).
38. R. Navawongse, H. Eichenbaum, *J. Neurosci.* **33**, 1002–1013 (2013).
39. H. Barbas, G. J. Blatt, *Hippocampus* **5**, 511–533 (1995).
40. T. Wolbers, J. M. Wiener, *Front. Hum. Neurosci.* **8**, 571 (2014).

ACKNOWLEDGMENTS

This work was supported by the National Institute of Mental Health (grant R01-MH076932) and the Wallenberg Network Initiative on Culture, Brain, and Learning. It was also made possible through the support of a grant from the John Templeton Foundation, "Prospective Psychology Stage 2: A Research Competition," to M. Seligman. The opinions expressed in this publication are those of the authors and do not necessarily reflect the views of the John Templeton Foundation. This work was additionally supported by fellowships from the NSF Graduate Research Fellowship Program, the NSF Integrative Graduate Education and Research Traineeship program, and the Natural Sciences and Engineering Research Council of Canada. Raw data are archived on the Stanford Neuroscience Institute server and will be made available upon request.

SUPPLEMENTARY MATERIALS

www.sciencemag.org/content/352/6291/1323/suppl/DC1
Materials and Methods
Supplementary Text
Figs. S1 to S6
References (*41*–*58*)

14 December 2015; accepted 12 May 2016
10.1126/science.aaf0784

NEURODEVELOPMENT

Oligodendrocyte heterogeneity in the mouse juvenile and adult central nervous system

Sueli Marques,[1]* Amit Zeisel,[1]* Simone Codeluppi,[1,2] David van Bruggen,[1] Ana Mendanha Falcão,[1] Lin Xiao,[3,4] Huiliang Li,[3] Martin Häring,[1] Hannah Hochgerner,[1] Roman A. Romanov,[1,5] Daniel Gyllborg,[1] Ana B. Muñoz-Manchado,[1] Gioele La Manno,[1] Peter Lönnerberg,[1] Elisa M. Floriddia,[1] Fatemah Rezayee,[1] Patrik Ernfors,[1] Ernest Arenas,[1] Jens Hjerling-Leffler,[1] Tibor Harkany,[1,5] William D. Richardson,[3] Sten Linnarsson,[1]† Gonçalo Castelo-Branco[1]†

Oligodendrocytes have been considered as a functionally homogeneous population in the central nervous system (CNS). We performed single-cell RNA sequencing on 5072 cells of the oligodendrocyte lineage from 10 regions of the mouse juvenile and adult CNS. Thirteen distinct populations were identified, 12 of which represent a continuum from *Pdgfra*$^+$ oligodendrocyte precursor cells (OPCs) to distinct mature oligodendrocytes. Initial stages of differentiation were similar across the juvenile CNS, whereas subsets of mature oligodendrocytes were enriched in specific regions in the adult brain. Newly formed oligodendrocytes were detected in the adult CNS and were responsive to complex motor learning. A second *Pdgfra*$^+$ population, distinct from OPCs, was found along vessels. Our study reveals the dynamics of oligodendrocyte differentiation and maturation, uncoupling them at a transcriptional level and highlighting oligodendrocyte heterogeneity in the CNS.

Oligodendrocytes ensheath axons in the central nervous system (CNS), allowing rapid saltatory conduction and providing metabolic support to neurons. Although a largely homogeneous oligodendrocyte population is thought to execute these functions throughout the CNS (*1*), these cells were originally described as morphologically heterogeneous (*2*). It is thus unclear whether oligodendrocytes become morphologically diversified during maturation through interactions within the local environment or whether there is intrinsic functional heterogeneity (*3*–*5*). We analyzed 5072 transcriptomes of single cells expressing markers from the oligodendrocyte lineage, isolated from 10 distinct regions of the anterior-posterior and dorsal-ventral axis of the mouse juvenile and adult CNS (Fig. 1, A and B). Biclustering analysis (*6*) (figs. S1B and S15), hierarchical clustering (Fig. 1C), and differential expression analysis (tables S1 and S2) led to the identification of 13 distinct cell populations. *t*-Distributed stochastic neighbor embedding (t-SNE) (Fig. 2A) supported by pseudotime analysis (fig. S2, A and B) indicated a narrow differentiation path connecting oligodendrocyte precursor cells (OPCs) and myelin-forming oligodendrocytes, which then diversify into six mature states.

Oligodendrocyte precursor cells coexpressed *Pdgfra* and *Cspg4* (Fig. 2B and figs. S1B and S10), and 10% coexpressed cell cycle genes (fig. S2, E and F), consistent with a cell division turnover of 19 days in the juvenile cortex (*7*). Several genes (such as *Fabp7* and *Tmem100*) identified in OPCs were previously associated with astrocytes and radial glia (*6*) (figs. S1B, S3, and S10), consistent with the origin of OPCs from radial glia–like cells, as well as their capacity to generate astrocytes in injury paradigms (*8*).

[1]Laboratory of Molecular Neurobiology, Department of Medical Biochemistry and Biophysics, Karolinska Institutet, SE-17177 Stockholm, Sweden. [2]Department of Physiology and Pharmacology, Karolinska Institutet, SE-17177 Stockholm, Sweden. [3]Wolfson Institute for Biomedical Research, University College London, Gower Street, London WC1E 6BT, UK. [4]Institute of Neuroscience, Second Military Medical University, 800 Xiangyin Road, Shanghai 200433, China. [5]Department of Molecular Neurosciences, Center for Brain Research, Medical University of Vienna, Vienna, Austria.
*These authors contributed equally to this work. †**Corresponding author. Email: sten.linnarsson@ki.se (S.L.); goncalo.castelo-branco@ki.se (G.C.-B.)**

Differentiation-committed oligodendrocyte precursors (COPs) were distinct from OPCs (because they lacked *Pdgfra* and *Cspg4*) and expressed *Neu4* and genes involved in keeping oligodendrocytes undifferentiated (*Sox6*, *Bmp4*, and *Gpr17*) (*9*–*11*) (Fig. 2B and figs. S1B, S4, and S10). COPs presented lower levels of cell cycle markers (fig. S2, E and F) while expressing genes involved in migration (*Tns3* and *Fyn*) (fig. S10). Newly formed oligodendrocytes (NFOL1 and NFOL2) expressed genes induced at early stages of differentiation (*Tcf7l2* and *Casr*) (fig. S10) (*12*–*14*). Whereas *Gpr17* expression decreased in these cells, we observed a peak in levels of *Tcf7l2*, which is involved in oligodendrocyte differentiation (fig. S10) (*15*).

Myelin-forming oligodendrocytes (MFOL1 and MFOL2) expressed genes responsible for myelin formation (*Mal*, *Mog*, *Plp1*, *Opalin*, and *Serinc5*) (fig. S1, A and B). Single-molecule fluorescence RNA in situ hybridization (smFISH) showed that myelin-forming populations (*Ctps*$^{+}$) were distinct from mature oligodendrocytes (*Klk6*$^{+}$) (Fig. 2C and fig. S4D). Mature oligodendrocytes (MOL1 to MOL6) expressed late oligodendrocyte differentiation genes (*Klk6* and *Apod*) (*12*), as well as genes present in myelinating cells (*Trf* and *Pmp22*) (fig. S1B).

We identified a second *Pdgfra*$^{+}$ population—vascular and leptomeningeal cells (VLMCs)—distinct from OPCs and segregated from all oligodendrocyte lineage cells (Figs. 1C and 2A). This population was also found when sorting green fluorescent protein (GFP)–positive cells from *Pdgfra*–histone 2B (H2B)–GFP (*16*) and *Pdgfra*-Cre-RCE (LoxP-GFP) mice (*17*) (fig. S2C). These cells exhibited low levels of *Cspg4* (NG2) (Fig. 2B) and specifically expressed *Lum* (Fig. 2B and fig. S4), markers of the pericyte lineage (*Vtn* and *Tbx18*) (Fig. 2B and figs. S1B and S2D), and laminins and collagens characteristic of the basal lamina. *Pdgfra*$^{+}$ and *Sox10*$^{-}$ VLMCs were localized on blood vessels (Fig. 2D and figs. S4 and S11, A and B) and meninges (fig. S11, A to C). In contrast, COL1A1^{-} and PDGFRA^{+} OPCs were distributed in the parenchyma, in close association but not overlapping with the vasculature (Fig. 2D and fig. S11B) (*18*). VLMCs specifically exhibited markers present in transcriptomes of OPCs isolated based on PDGFRA^{+} immunoreactivity (fig. S3) (*14*), most likely previously assigned to OPCs due to copurification.

We retrieved the 50 genes that better differentiate every branch of the dendrogram plot (Fig. 1C) and investigated their putative function by gene ontology analysis (figs. S6 to S9 and tables S1 and S2). COPs were enriched in cell fate commitment and adhesion genes, whereas newly formed oligodendrocytes (NFOL1 and NFOL2) already presented genes involved in steroid biosynthesis, ensheathment of neurons, and cell projection organization (fig. S7). These populations exhibited distinct expression of *Tcf7l2*, *Itpr2*, *Tmem2*, and *Pdgfa* (Fig. 3A and fig. S4). ITPR2, encoding an intracellular Ca^{2+} channel, was more specific to oligodendrocytes than TCF7L2 and exhibited close to 100% overlap with SOX10-positive cells (fig. S5, A and D). We observed that

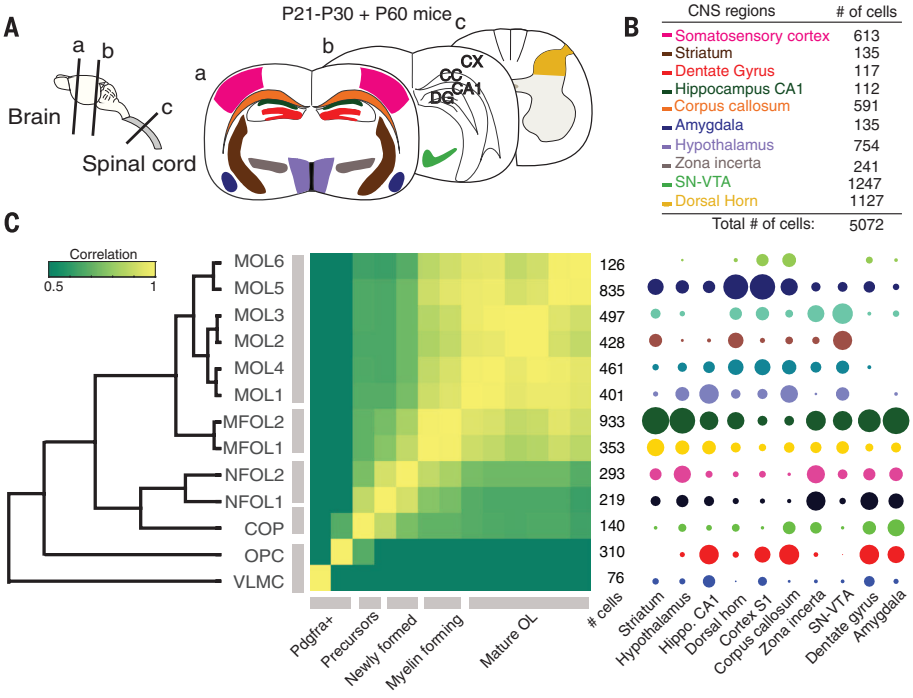

Fig. 1. Single-cell RNA sequencing analysis of 5072 cells expressing markers of the oligodendrocyte lineage in 10 regions of the mouse CNS. (**A**) Targeted regions. CX, cortex; CC, corpus callosum; CA1, CA1 hippocampus; DG, dentate gyrus. (**B**) Number of cells analyzed for each region. SN-VTA, substantia nigra ventral tegmental area. (**C**) Hierarchical clustering (left), correlation matrix (middle), and subclass abundances by region (right). OL, oligodendrocytes.

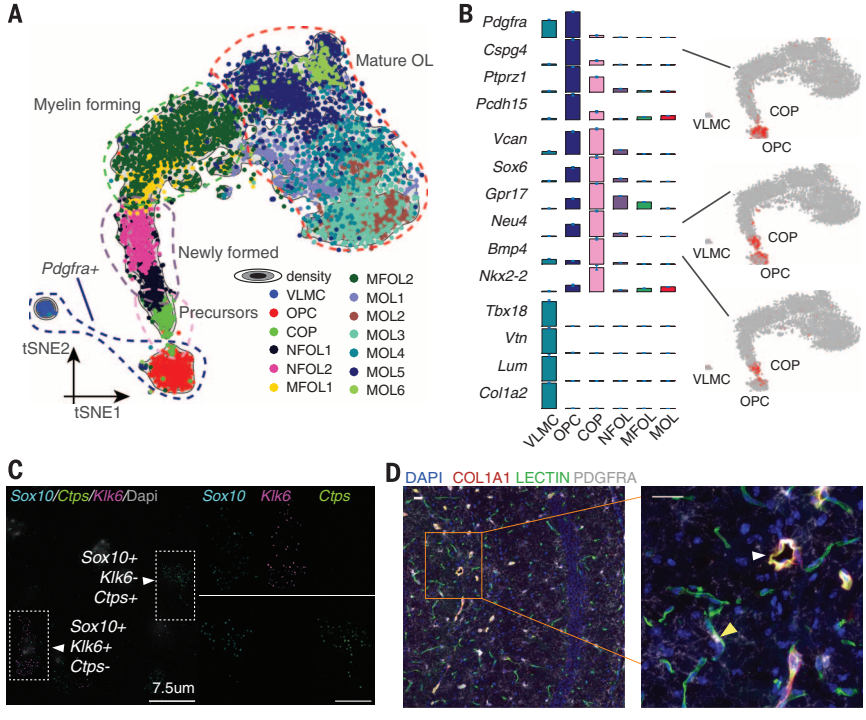

Fig. 2. Oligodendrocyte cell states in the continuous maturation process from precursors to mature cells. (**A**) *t*-Distributed stochastic neighbor embedding projection showing the trajectory from OPCs to mature oligodendrocytes. (**B**) Average (±SEM) expression of marker genes for OPCs, COPs, and VLMCs. Representative markers are overlaid on the t-SNE map (gray, low expression; red, high expression). (**C**) Results of smFISH for *Sox10*, *Ctps* (MFOL marker), and *Klk6* (MOL marker) confirm that these populations are distinct. DAPI, 4′,6-diamidino-2-phenylindole. Scale bar, 7.5 μm. (**D**) Immunohistochemistry of COL1A1 (VLMCs), PDGFRA (OPCs and VLMCs), and Tomato LECTIN (blood vessels) in the brain at P21. White arrowhead, VLMCs; yellow arrowhead, OPCs (COL1A1^{-}). Scale bars, 25 μm.

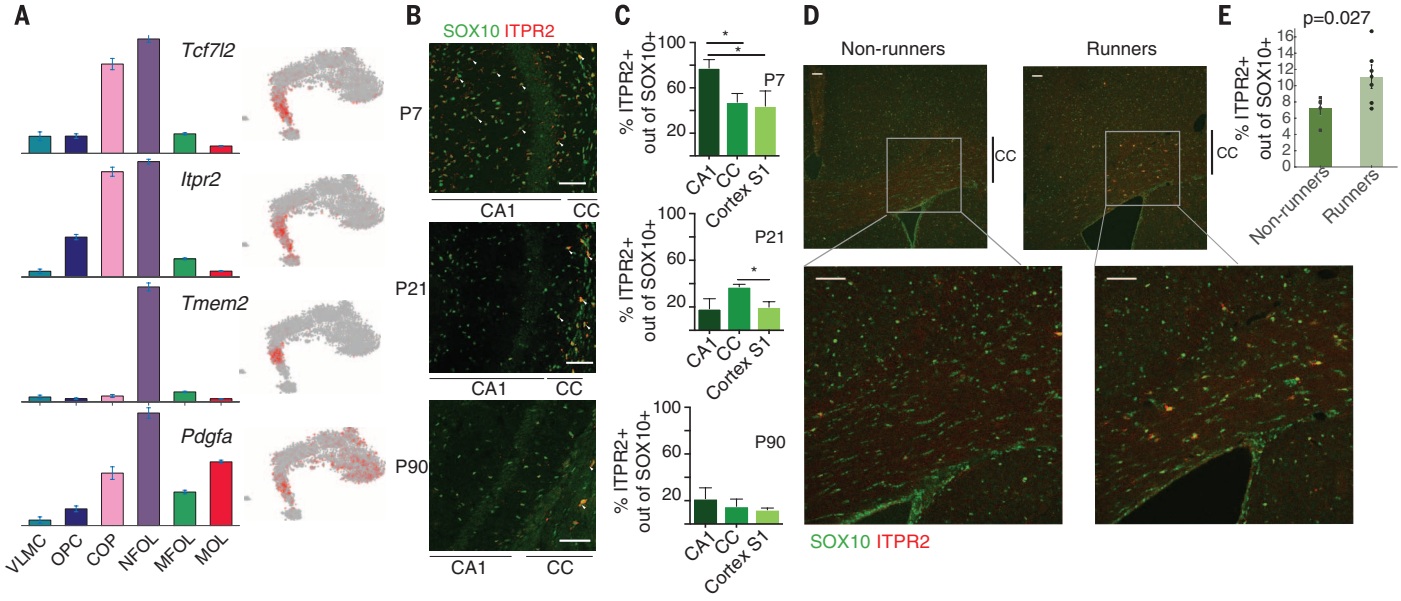

Fig. 3. ITPR2$^+$ oligodendrocytes are present in regions of active differentiation and increase in mice undergoing learning in the complex wheel paradigm. (**A**) Average (±SEM) expression level of *Tcf7l2*, *Itpr2*, *Tmem2*, and *Pdgfa* along the oligodendrocyte lineage. (**B** and **C**) Immunohistochemistry and quantification of ITPR2$^+$ out of SOX10$^+$ cells in the brain at P7, P21, and P90. One-way analysis of variance with Tukey's multiple comparison test (*$P < 0.05$, $n = 3$ mice per time point). Error bars indicate SEM. (**D** and **E**) Immunohistochemistry and quantification of ITPR2$^+$ out of SOX10$^+$ cells in the corpus callosum of P60 nonrunners (squares) versus runners (circles) after 2 days in the complex wheel-learning paradigm (one-tailed Student's *t* test). Scale bars in (D), 75 μm. Error bars in (E) indicate SEM.

ITPR2 immunoreactive cells were distinct from PDGFRA$^+$ OPCs (fig. S5B), and lineage tracing confirmed that ITPR2$^+$ cells are the progeny of OPCs (figs. S2C and S5C). Of the OPC-derived *Pdgfra*-H2B-GFP$^+$ cells, 22 ± 2 and 25 ± 1.5% were positive for ITPR2 in the somatosensory (S1) cortex and the CA1 hippocampus, respectively, at postnatal day 21 (P21), whereas 43 ± 3.7% double-positive cells were found in the corpus callosum (fig. S5C). The percentage of ITPR2$^+$, Sox10$^+$ cells in the corpus callosum remained within the same range at P7 (47 ± 4%) and P21 (37 ± 1%) (Fig. 3C). Of the SOX10$^+$ oligodendrocytes, 77 ± 4 and 48 ± 7% were positive for ITPR2 at P7 in the CA1 hippocampus and the S1 cortex, respectively, and decreased to less than 20% thereafter (Fig. 3, B and C). This distribution of ITPR2$^+$ oligodendrocytes correlates with active and prolonged differentiation in the juvenile rat corpus callosum (*19*). These tissues still maintained 10 to 20% ITPR2$^+$ cells at adult stages (P90 in Fig. 3C).

To investigate the potential function of ITPR2$^+$ cells in the adult brain, we analyzed their dynamics in the corpus callosum of mice engaged in motor learning on the complex wheel, a process that requires active myelination (*20*). In this paradigm, running on the wheel leads to an increase in the number of proliferating OPCs after 4 days, followed by an increase in oligodendrocytes after 8 days (*20*). However, increased motor skills were already apparent after 2 days in wild-type mice, but not in mutant mice that were unable to synthesize new myelin (*20*), suggesting that oligodendrocyte lineage cells already contribute to learning within the first 2 days. We found that the number of ITPR2$^+$, SOX10$^+$ cells increased by ~50% in mice that ran on the complex wheel for 2 days, as compared with nonrunners (Fig. 3, D and E). Thus, novel motor activity might trigger rapid differentiation of OPCs into ITPR2$^+$ committed precursors and newly formed oligodendrocytes that contribute to early learning by facilitating electrical transmission, either through the initiation of myelination or some other pre-myelinating function.

We were unable to identify region- or age (juvenile versus adult)–specific subpopulations of OPCs in our data set (Figs. 2A and 4, A and B). Nevertheless, 16% of the juvenile OPCs were in the cell cycle [as determined by the simultaneous expression of more than two cell cycle markers (fig. S2F)], compared with ~3% of the adult OPCs. Similarly, COPs and newly formed oligodendrocytes were present in all regions in juvenile mice (Figs. 1C and 4A), revealing a common trajectory of differentiation between the various regions (Fig. 2A). These populations were also observed in the adult corpus callosum and the S1 cortex, albeit in considerably lower numbers compared with those seen in juvenile mice (Fig. 4B). On the basis of the distribution of cell types in the juvenile mice, we classified regions as immature (anterior regions such as the amygdala and hippocampus), intermediate (corpus callosum, zona incerta, striatum, and hypothalamus), and mature (cortex and posterior regions such as the dorsal horn and the substantia nigra ventral tegmental area) (Fig. 4A and fig. S12). These regional variations could result from different timing of oligodendrocyte maturation during postnatal development (*21*, *22*). Myelination first starts in the rat in posterior regions (dorsal horn) around P7, whereas in anterior regions of the CNS (amygdala, hippocampus, striatum, and cortex) it occurs between P21 and P28 (*23*).

Different regions of the CNS were populated by diverse mature oligodendrocytes (Fig. 1C and fig. S12). Although some populations, such as MOL5, were present throughout the regions, other mature oligodendrocytes were enriched in certain regions (fig. S12). Some of these mature oligodendrocyte populations might be intermediate stages or have specific functions in juvenile mice but then disappear in adulthood. Subsets of MOL5 and MOL6 were mainly present in the S1 cortex and corpus callosum in the adult mice (Fig. 4B). Because MOL5 was already present in several regions of the juvenile CNS (Fig. 1C and fig. S12), final maturation of oligodendrocytes might already be achieved in the juvenile mice in certain regions, such as the dorsal horn, but only in adulthood in others, such as the corpus callosum.

Gene ontology analysis indicated a divergence already at the stage of myelin formation (fig. S8 and tables S1 and S2). Although mature oligodendrocyte populations shared the expression of many genes, some were differentially enriched within populations (fig. S8 and tables S1 and S2), indicating segregation of MOL1 to MOL4, enriched in lipid biosynthesis and myelination genes (*Far1* and *Pmp22*) from MOL5 and MOL6 (adult), enriched for synapse parts such as *Grm3* (metabotropic glutamate receptor, mainly enriched in MOL6) and *Jph4*. We confirmed the presence of GRM3 in the oligodendrocyte lineage (*Pdgfra*-Cre-RCE) and specifically in CC1$^+$ mature oligodendrocytes in the juvenile cortex (fig. S11D). Even within MOL1 to MOL4, which were enriched

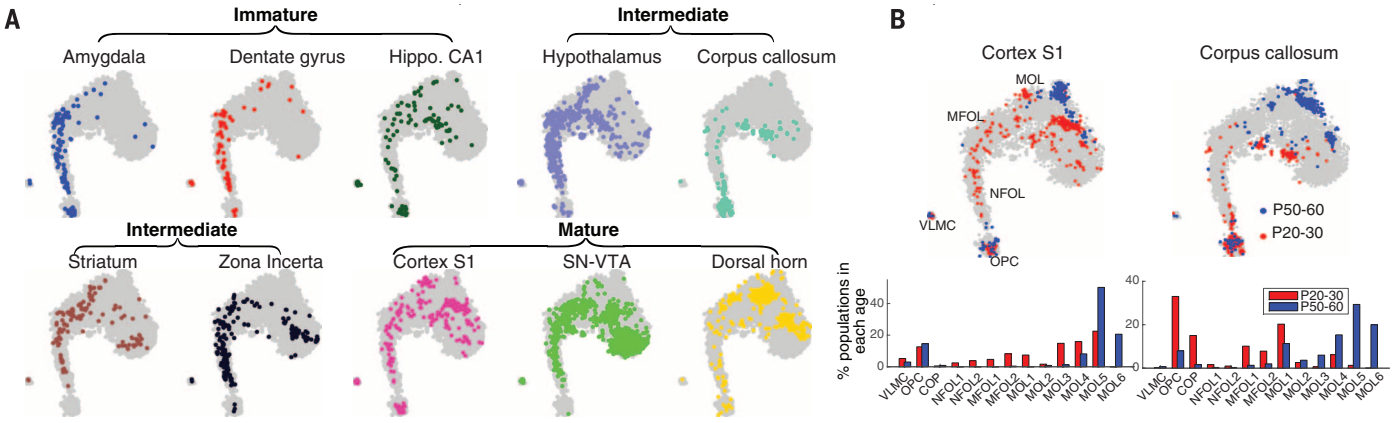

Fig. 4. Region- and age-specific distribution of mature oligodendrocytes. (**A**) *t*-Distributed stochastic neighbor embedding projections, as in Fig. 2A, with colored dots representing cells from each of the 10 CNS regions analyzed. (**B**) Age distribution of oligodendrocyte populations in the S1 cortex and corpus callosum. Bar plots show the percentage of each population by age. Red, juvenile brain; blue, adult brain.

in myelin-related genes, specific populations (such as MOL3) are more likely to be involved in synaptic activity (fig. S9 and tables S1 and S2). Optic nerve oligodendrocytes can form axon-myelinic synapses, responding to axonal action potentials via glutamate ionotropic *N*-methyl-D-aspartate receptors (*24*). We analyzed the expression of ionotropic and metabotropic glutamate receptors and other ion channels, including transient receptor potential (TRP) (*25*) and potassium channels (fig. S14). Although most glutamate receptor subunits were expressed throughout oligodendrocyte lineage cells, there was preferential expression in some populations, with single cells displaying combinations of subunits that might determine function. Potassium channels and TRPs were also expressed in a cell type–specific manner, displaying a scattered distribution within populations (fig. S14). Thus, the communication of mature oligodendrocytes with neighboring neurons might be mediated through specific receptors and channels, following synaptic input or vesicular release.

Our study provides a high-resolution view of the transcriptional landscape of a single neural subtype across multiple regions of the CNS and indicates a transcriptional continuum between oligodendrocyte populations, with a subset representing distinct but nevertheless connected stages in the maturation path from OPCs to mature oligodendrocytes (fig. S16). Initial differentiation was uniform throughout the CNS, whereas mature oligodendrocyte subtype specification occurred later at postnatal stages and in a region-specific manner. Each brain region appears to optimize its circuitry by representation of distinct proportions and combinations of mature oligodendrocytes. Our data also indicate that ITPR2$^+$ oligodendrocytes are involved in rapid myelination in complex motor learning and thus might be relevant in other active maturation and myelination processes, such as remyelination in disease or lesion paradigms. Nonproliferative *Nkx2.2*$^+$ precursors that have a profile consistent with these cells (fig. S10) have been observed in lesions of patients with multiple sclerosis (*26*). Therefore, by establishing oligodendrocytes as a transcriptionally heterogeneous cell lineage, our study might lead to new insights into the etiology of myelin disorders, such as multiple sclerosis, and might suggest novel targets for their treatment.

REFERENCES AND NOTES

1. N. Kessaris *et al.*, *Nat. Neurosci.* **9**, 173–179 (2006).
2. P. d. Rio-Hortega, *Mem. Real Soc. Esp. Hist. Nat.* **14**, 5–122 (1928).
3. G. S. Tomassy *et al.*, *Science* **344**, 319–324 (2014).
4. R. B. Tripathi *et al.*, *J. Neurosci.* **31**, 6809–6819 (2011).
5. M. E. Bechler, L. Byrne, C. Ffrench-Constant, *Curr. Biol.* **25**, 2411–2416 (2015).
6. A. Zeisel *et al.*, *Science* **347**, 1138–1142 (2015).
7. K. M. Young *et al.*, *Neuron* **77**, 873–885 (2013).
8. L. Dimou, M. Götz, *Physiol. Rev.* **94**, 709–737 (2014).
9. C. C. Stolt *et al.*, *Dev. Cell* **11**, 697–709 (2006).
10. J. Samanta, J. A. Kessler, *Development* **131**, 4131–4142 (2004).
11. Y. Chen *et al.*, *Nat. Neurosci.* **12**, 1398–1406 (2009).
12. J. D. Cahoy *et al.*, *J. Neurosci.* **28**, 264–278 (2008).
13. V. A. Swiss *et al.*, *PLOS ONE* **6**, e18088 (2011).
14. Y. Zhang *et al.*, *J. Neurosci.* **34**, 11929–11947 (2014).
15. F. Ye *et al.*, *Nat. Neurosci.* **12**, 829–838 (2009).
16. R. A. Klinghoffer, T. G. Hamilton, R. Hoch, P. Soriano, *Dev. Cell* **2**, 103–113 (2002).
17. K. Roesch *et al.*, *J. Comp. Neurol.* **509**, 225–238 (2008).
18. H. H. Tsai *et al.*, *Science* **351**, 379–384 (2016).
19. K. Hamano *et al.*, *Brain Res. Dev. Brain Res.* **108**, 287–293 (1998).
20. I. A. McKenzie *et al.*, *Science* **346**, 318–322 (2014).
21. H. C. Kinney, B. A. Brody, A. S. Kloman, F. H. Gilles, *J. Neuropathol. Exp. Neurol.* **47**, 217–234 (1988).
22. B. A. Brody, H. C. Kinney, A. S. Kloman, F. H. Gilles, *J. Neuropathol. Exp. Neurol.* **46**, 283–301 (1987).
23. J. C. Coffey, K. W. McDermott, *J. Neurocytol.* **26**, 149–161 (1997).
24. I. Micu *et al.*, *Exp. Neurol.* **276**, 41–50 (2016).
25. N. B. Hamilton, K. Kolodziejczyk, E. Kougioumtzidou, D. Attwell, *Nature* **529**, 523–527 (2016).
26. T. Kuhlmann *et al.*, *Brain* **131**, 1749–1758 (2008).

ACKNOWLEDGMENTS

We thank P. Soriano (Mount Sinai, New York) for the *Pdgfra*-H2B-GFP mouse; C. Göritz for discussions; and Samudyata, G. Chen, A. Nanni, and J. Söderlund for additional support.

P.E. was supported by the Swedish Research Council (VR) (Medicine and Health), the Swedish Cancer Society, and the Wallenberg Scholar and Söderberg Foundation. E.A. was supported by VR (Linnaeus Center in Developmental Biology for Regenerative Medicine, grants 2011-3116 and 2011-3318), the Swedish Foundation for Strategic Research (Successful Research Leaders program), the European Union (EU) (NeuroStemCellRepair and DDPDGENES), and the Karolinska Institutet (KI) (SFO Stem Cells and Regenerative Medicine). J.H.-L. was supported by VR, StratNeuro, Hjärnfonden, and EU FP7/Marie Curie Actions. R.A.R. was supported by the European Molecular Biology Organization (ALTF reference 596-2014) and EU FP7 (Marie Curie Actions, EMBOCOFUND2012, grant GA-2012-600394). T.H. was supported by VR, Hjärnfonden, the Petrus and Augusta Hedlunds Foundation, the Novo Nordisk Foundation, the European Research Council (ERC) (SECRET-CELLS), and the EU (PAINCAGE). W.D.R. was supported by the ERC (grant 293544) and the Wellcome Trust (grants 100269/Z/12/Z and 108726/Z/15/Z). L.X. was supported by the National Natural Science Foundation of China (grant 31471013). H.L. was supported by a New Investigator Award from the UK Biotechnology and Biological Sciences Research Council (BB/L003236/1). A.Z. was supported by the Human Frontier Science Program. S.L. was supported by the ERC (BRAINCELL grant 261063), VR (STARGET), the Wellcome Trust (grant 108726/Z/15/Z), and the EU (FP7/DDPDGENES). A.M.F. was supported by the European Committee for Treatment and Research of Multiple Sclerosis. G.C.-B. was supported by VR (grant 2015-03558), the EU (FP7/Marie Curie Integration Grant, EPIOPC), Hjärnfonden, the Swedish Society of Medicine, Åke Wiberg, Clas Groschinsky, the Petrus och Augusta Hedlunds Foundations, and KI. Data sets were deposited in the Gene Expression Omnibus (accession no. GSE75330) and in a web interface at http://linnarssonlab.org/oligodendrocytes/. The supplementary materials contain additional data. S.M., A.Z., H.L., W.D.R., S.L., and G.C.-B. designed the experiments. P.E., E.A., J.H.-L., T.H., W.D.R., S.L., and G.C.-B. (senior authors) obtained funding. S.M., A.Z., S.C., H.H., R.A.R., D.G., M.H., A.B.M.-M., G.L.M., F.R., H.L., L.X., and E.M.F. performed experiments. L.X., H.L., and W.D.R. have priority of observation of the rapid differentiation of oligodendrocytes in the complex motor wheel paradigm. S.M., A.Z., D.v.B., A.M.F., G.L.M., and P.L. analyzed the data. S.M., A.Z., S.L., and G.C.-B. wrote the paper, with the assistance of and proofreading by all authors.

SUPPLEMENTARY MATERIALS

www.sciencemag.org/content/352/6291/1326/suppl/DC1
Materials and Methods
Figs. S1 to S16
Tables S1 to S3
References (*27*–*34*)

9 March 2016; accepted 10 May 2016
10.1126/science.aaf6463

Oligodendrocyte heterogeneity in the mouse juvenile and adult central nervous system

Sueli Marques, Amit Zeisel, Simone Codeluppi, David van Bruggen, Ana Mendanha Falcão, Lin Xiao, Huiliang Li, Martin Häring, Hannah Hochgerner, Roman A. Romanov, Daniel Gyllborg, Ana B. Muñoz-Manchado, Gioele La Manno, Peter Lönnerberg, Elisa M. Floriddia, Fatemah Rezayee, Patrik Ernfors, Ernest Arenas, Jens Hjerling-Leffler, Tibor Harkany, William D. Richardson, Sten Linnarsson and Gonçalo Castelo-Branco (June 9, 2016)
Science **352** (6291), 1326-1329. [doi: 10.1126/science.aaf6463]

Editor's Summary

One size does not fit all

Oligodendrocytes are best known for their ability to myelinate brain neurons, thus increasing the speed of signal transmission. Marques *et al.* surveyed oligodendrocytes of developing mice and found unexpected heterogeneity. Transcriptional analysis identified 12 populations, ranging from precursors to mature oligodendrocytes. Transcriptional profiles diverged as the oligodendrocytes matured, building distinct populations. One population was responsive to motor learning, and another, with a different transcriptome, traveled along blood vessels.

Science, this issue p. 1326

Science (print ISSN 0036-8075; online ISSN 1095-9203) is published weekly, except the last week in December, by the American Association for the Advancement of Science, 1200 New York Avenue NW, Washington, DC 20005.